Int J Thermophys (2007) 28:1646–1652
DOI 10.1007/s10765-007-0292-x

Microstructure and Thermal Diffusivity of Ceramic Powders

G. Peña-Rodríguez · J. A. I. Díaz Gongora · R. A. Muñoz-Hernández · J. L. Fernández Muñoz · E. Marín · A. Calderón

Published online: 30 October 2007
© Springer Science+Business Media, LLC 2007

Abstract For the first time, the thermal diffusivity (α) in red clay samples has been determined as a function of the annealing time, for a furnace temperature above 900°C. The thermal diffusivity measurements on the samples were obtained by means of the photoacoustic technique in a heat transmission configuration. A complementary microstructure analysis using X-ray diffraction (XRD) and energy dispersion spectroscopy (EDS) has been performed. The ceramic material used in this work is widely used in the fabrication of several kinds of building materials such as bricks and roof tiles in the north oriental region of Colombia (Cúcuta). The importance of these results is in the determination of conditions to obtain manufactured products with the desired heat transport capacity.

Keywords Ceramic powders · Microstructure · Thermal diffusivity

Paper presented at the Seventeenth European Conference on Thermophysical Properties, September 5–8, 2005, Bratislava, Slovak Republic.

G. Peña-Rodríguez
Departamento de Física, Universidad Francisco de Paula
Santander A. A., Cúcuta 1055, Colombia

J. A. I. Díaz Gongora · R. A. Muñoz-Hernández ·
J. L. Fernández Muñoz · E. Marín · A. Calderón (✉)
Centro de Investigación en Ciencia Aplicada y
Tecnología Avanzada del IPN, Legaria 694
Colonia Irrigación, México D.F. 11500, México
e-mail: jcalderona@ipn.mx

Present Address:
E. Marín
Facultad de Física, Universidad de La Habana, San Lázaro y L,
Vedado, La Habana 10400, Cuba

1 Introduction

Grain-shaped materials are important in industries owing to their wide range of applications. This is the case for ceramic powders and their applications in the building materials industry. However, studies about their thermal properties as a function of manufacturing parameters such as annealing time and chemical composition are very rare [1]. The thermal diffusivity (α) is a significant and useful thermophysical parameter because it is a unique characteristic for each material, and it represents the heat flux rate through a medium [2]. Variations of this thermal transport parameter depend on changes in the composition and/or structure of the material [3].

The photoacoustic (PA) technique has proved to be a powerful tool for determination of α in a wide variety of materials [4–6]. In our experimental setup, a laser light beam is modulated at a frequency f before it normally impinges on the surface of the sample, which is placed in contact with the front chamber of an electret microphone. Finally, the data of amplitude and phase of the detected signal are recorded as a function of the modulation frequency [5].

In the surroundings of San José de Cúcuta, in the northern region of Colombia, there are red clay fields, which are the main source for the ceramic factories in the zone that manufactures bricks, floor tiles, roof tiles, wall tiles, etc. In this work we report, for the first time, the determination of the thermal diffusivity in these red clay samples as a function of the annealing time, for a furnace temperature above 900°C. In addition, we performed a complementary microstructure analysis using X-ray diffraction (XRD) and energy dispersion spectroscopy (EDS).

2 Experimental Details

2.1 Samples

We used red clay powders from the Tejar Los Vados region, to prepare the samples in the form of pills. Then the samples were put into a furnace (1400 Thermolyne) to 900°C for periods of 0, 30, 60, 90, 120, and 150 min. The heating temperature was chosen because the red clay products are fabricated between 850 and 1,000°C [7]. In Table 1, the sample thicknesses measured with a digital micrometer (Mitutoyo, Model 543-692) are given.

Table 1 Thickness, cut frequency, and measured thermal diffusivity of the red clay samples

Sample	l (μm)	f_c (Hz)	α (10^{-3}cm$^2\cdot$s^{-1})
M0-0	300 ± 3	0.582 ± 0.004	1.69 ± 0.04
M0-30	300 ± 5	0.915 ± 0.007	2.59 ± 0.11
M0-60	319 ± 3	0.716 ± 0.004	2.29 ± 0.06
M0-90	290 ± 5	1.070 ± 0.006	2.83 ± 0.11
M0-120	295 ± 5	0.872 ± 0.004	2.38 ± 0.09
M0-150	236 ± 4	1.338 ± 0.004	2.34 ± 0.09

2.2 Thermal-Diffusivity Determination

For a modulation frequency f given, the thermal diffusion length $\mu_\alpha = (\alpha_s/\pi f)^{1/2}$ is the distance at which the PA signal amplitude decays to 1/e = 0.368 of its initial value. In a sample with thermal diffusivity and thickness given by α_s and l_s, respectively, the "cut frequency," which represents the modulation frequency at which the thermal diffusion length matches the sample thickness, is given by

$$f_c = \alpha/\pi l^2 \tag{1}$$

From the one-dimensional thermal diffusion model, the amplitude of the PA signal, for optically opaque and thermally thick samples ($\mu_\alpha \ll l_s$), is given as [4–6]

$$A = cte\frac{1}{f}\exp(-\sqrt{f/f_c}) \tag{2}$$

Here, *cte* is a parameter that depends on the pressure, thermal properties of the air inside the acoustic chamber, light intensity, and photoacoustic cell geometry. The cut frequency f_c can be obtained by fitting Eq. 2 to signal data amplitudes [4–6], and then by means of Eq. 1, the thermal diffusivity of the sample is obtained.

2.3 Microstructure

A Siemmens D-5000 diffractometer was used in this study. The full width height medium (FWHM) was analyzed with the PowderX software. Moreover, we used a scanning electron microscope (Philips ESEM-XL30) in order to obtain the elementary chemical analysis in the samples.

3 Results and Discussion

3.1 Thermal Diffusivity

In Table 1, the results of the cut frequency and thermal diffusivity are shown for each sample. Figure 1 shows the PA signal amplitude versus modulation frequency for the sample M0-150; the curve indicates the best fit of Eq. (2) to the experimental data. In Fig. 2, we present α as a function of the annealing time for the six samples. We observed an increase in α with the annealing time until reaching a maximum at 90 min, and then α decreases with the annealing time. The maximum value of a α (2.83×10^{-3} cm^2·s^{-1}) corresponds to a 67% increase from α for the sample without thermal treatment (1.69×10^{-3} cm^2·s^{-1}). A comparison of the values in Table 1 and reported values for materials such as bricks (2.78×10^{-3} cm^2·s^{-1}) [2] and roof tiles (1.49×10^{-3} cm^2·s^{-1}) [8] shows similar values.

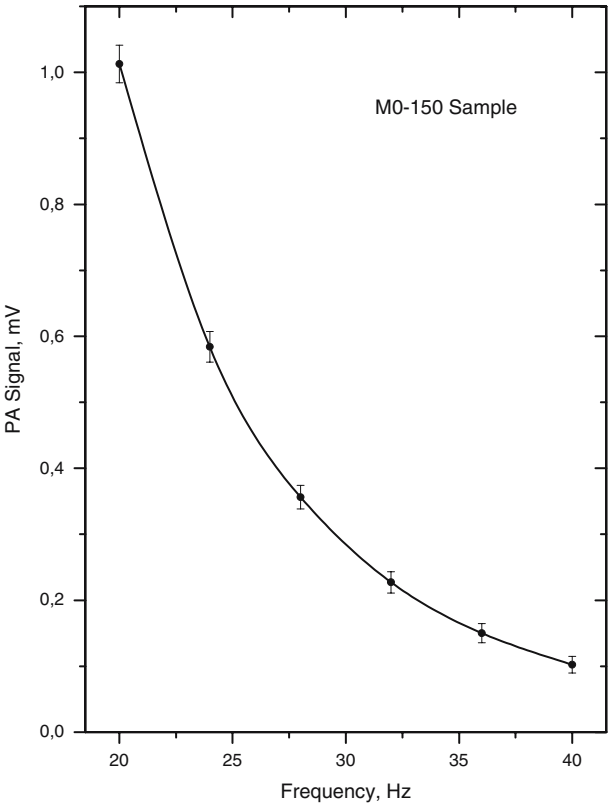

Fig. 1 PA signal amplitude versus modulation frequency for the sample M0-150, the curve indicates the best fit of Eq. 2 to the experimental data

3.2 XRD Analysis

Figure 3 shows the XRD patterns for the six samples. The higher intensity peaks for all the samples are placed in the same diffraction angles and the FWHM shows no variation with the annealing time of the samples; there is no crystallization process in the samples. The principal crystal phases are from: (Al_2O_3), ($K_{6.8}Si_{45.3}$), (Fe_2O_3), (SiO_2), and (Fe_2SiO_4). There is no significant difference in composition by mass among samples made with different annealing times. The elements present in a larger quantity are: silicon, oxygen, and aluminum, which correspond to the elements in the chemical composition of red clay.

3.3 EDAX Analysis

Table 2 shows results of the energy dispersive X-ray analysis (EDAX) for the M0-0 sample. Elementary chemical analysis shows a smaller proportion of iron (Fe) and potassium (K). These elements are important since they are components of

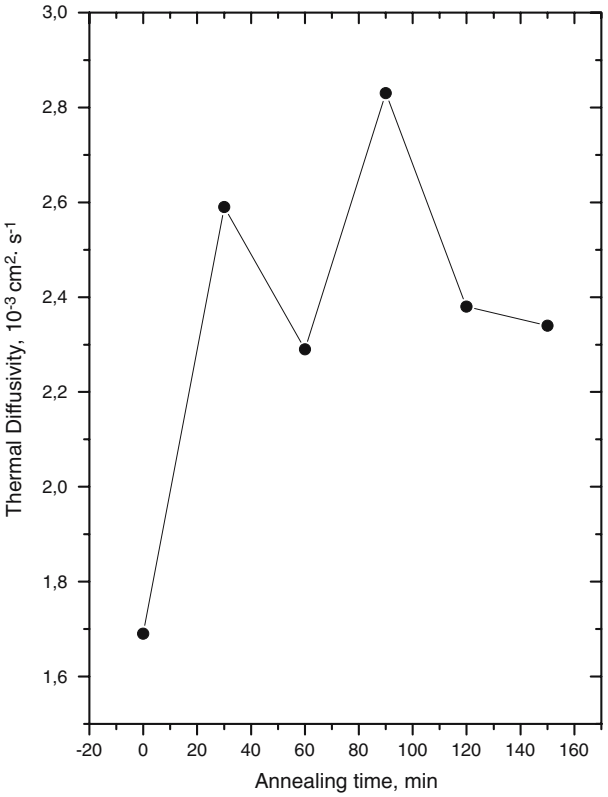

Fig. 2 Thermal diffusivity versus annealing time for red clay samples

compounds such as iron oxide (Fe_2O_3), iron silicate (Fe_2SiO_4), and potassium silicate ($K_{6.8}Si_{45.3}$), which are in the studied samples, obtained from qualitative analysis by means of XRD. Finally, we do not obtain any significant difference for the analysis by EDAX among all the samples.

4 Conclusions

We determined the thermal diffusivity (α) in red clay samples, as a function of the annealing time of their elaboration process which was carried out at a constant temperature, above 900°C. Our results show a dependence between measured α values and the annealing time, in such a way that α values are in the range ($1.69–2.83 \times 10^{-3} cm^2 \cdot s^{-1}$) and α increases with the annealing time until reaching a maximum value at 90 min ($2.83 \times 10^{-3} cm^2 \cdot s^{-1}$), corresponding to a 67% increase compared to the sample without thermal treatment ($1.69 \times 10^{-3} cm^2 \cdot s^{-1}$), and then α decreases with the annealing time. These results show that the sample with 90 min of annealing time for a furnace temperature above 900°C has the maximum thermal transport capacity, which is important to know in the fabrication of building materials with this material. On the other

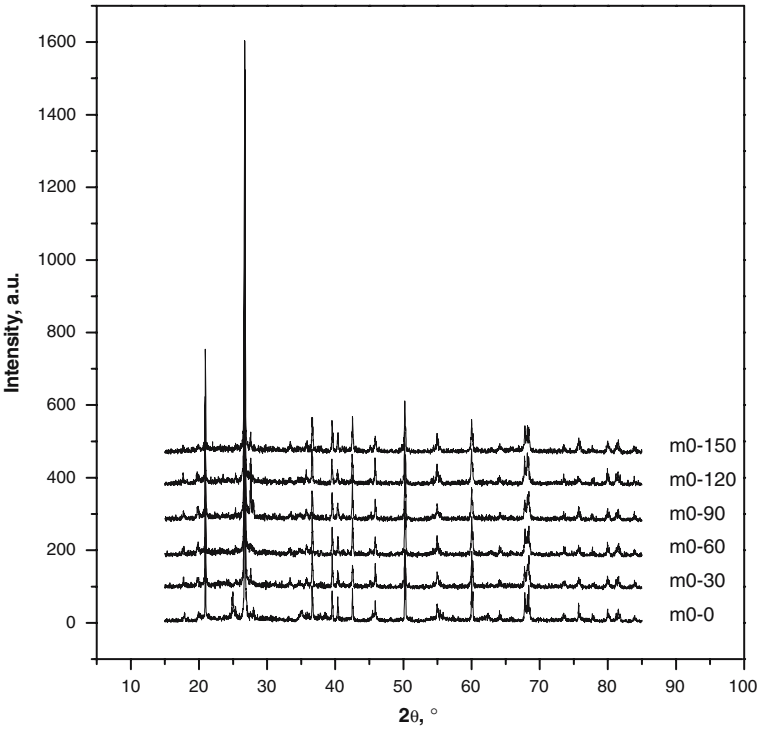

Fig. 3 XRD patterns for samples

Table 2 Elemental chemical composition of M0-0 sample

Element	Mass%	Mol%
O	38.09	52.9
Mg	0.80	0.73
Al	13.67	11.26
Si	39.99	31.64
K	2.78	1.58
Ti	0.57	0.26
Fe	4.11	1.63
Total	100	100

hand, XRD analysis shows that the principal crystal phases are: (Al_2O_3), ($K_{6.8}Si_{45.3}$), (Fe_2O_3), (SiO_2), and (Fe_2SiO_4). EDAX analysis show that the red ceramic powders are mostly composed of O, Si, Al, Fe, and K. Finally, we observe no significant difference in mass for the composition among samples treated with different annealing times.

References

1. G.D. Ladiwala, K.N. Bala, S. Saxena, M.P. Saksena, in *Proceedings of the 22nd International Conference on Thermal Conductivity,* vol. 22, ed. by Timothy W. Tong (Technomic Publishing Co., Lancaster, Pennsylvania, 1994)

2. Y.S. Touloukian, R.W. Powell, C.Y. Ho, M.C. Nicolaou, *Thermophysical Propieties of Matter*, vol. 10 (Plenum, New York, 1970)
3. A. Calderón, J.J. Alvarado, Y.G. Gurevich, A. Cruz Orea, I. Delgadillo, H. Vargas, L.C.M. Miranda, Phys. Rev. Lett. **79**, 5022 (1997)
4. M.V. Marquezini, M.N. Cella, A.M. Mansanares, H. Vargas, L.C.M. Miranda, Meas. Sci. Technol. **2**, 396 (1991)
5. G. Peña Rodríguez, A. Calderón Arenas, R.A. Muñoz Hernández, S. Stolik, A. Cruz Orea, F. Sánchez Sinencio, Anal. Sci. **17**, s357 (2001)
6. A.M. Manzanares, A.C. Bento, H. Vargas, N.F. Leite, L.C.M. Miranda, Phys. Rev. B **42**, 4477 (1990)
7. http://www.emison.com/215.htm
8. F.P. Incropera, D.P. Dewitt. *Fundamentos de transferencia de calor*, 4th edn. (Prentice-Hall, México, 1999)